INFLUENCE OF HALL CURRENTS ON THE CASSON FLUID FLOW DUE TO AN EXPONENTIALLY STRETCHING SHEET WITH SUCTION AND CONVECTIVE BOUNDARY CONDITION

VASUNDHARA B[1], SAROJAMMA G[2,*], SREELAKSHMI K[3], VIJAYA N[4]

**[1, 2, 3, 4] Department of Applied Mathematics
Sri Padmavati Mahila Visvavidyalayam, Tirupati-517502, India.**

ABSTRACT

In this paper the effects of suction, thermal radiation, heat generation on the unsteady flow of a Casson fluid over an exponentially stretching sheet in the presence of Hall currents with convective boundary condition is investigated. The governing equations of the flow are formulated and solved numerically on introducing suitable similarity transformations. The computational results indicate that the magnetic field acts as a resisting force on the primary velocity while it has an opposite influence on the secondary velocity. The Biot number and thermal radiation parameter enhance the temperature. The rate of mass transfer is reduced with Schmidt number.

Keywords: Casson fluid, convective boundary condition, Exponentially stretching sheet.

1 INTRODUCTION

Magyari and Keller (1999) are the first researchers to analyse the free convection flow, heat and mass transfer of an incompressible viscous fluid from an exponentially stretching vertical surface. They obtained similarity solutions pertaining to an exponential stretching and exponential temperature of the continuous surface. Following this study, several researchers studied the laminar boundary layer flow and heat transfer of a viscous fluid over an exponentially stretching surface under different conditions. The study of non-Newtonian fluids due to an exponential stretching sheet finds applications in chemical industry. Nadeem *et al.* [2011] analyzed the effect of thermal radiation on the boundary layer flow of a Jeffery fluid past an exponentially stretching surface. Pavithra and Gireesha [2013] made a numerical study of the boundary layer flow and heat transfer of a dusty fluid over an exponentially stretching surface taking into account the viscous dissipation and internal heat generation and absorption. Anwar *et al.* [2014] analysed the unsteady MHD mixed convective boundary layer flow of a nanofluid over an exponentially stretching sheet in porous media. Nadeem and Hussain [2014] investigated the heat transfer of a pseudo plastic fluid past an exponentially porous stretching surface modelling as a Williamson fluid. Convective heat transfer is of the excessive significance in procedures in which high temperatures are involved. For example, gas turbines, nuclear plants, storage of thermal energy etc. Referring to numerous industrial and engineering processes the convective boundary conditions are more practical including material drying, transpiration cooling process etc. Nadeem *et al* [2014] investigated the steady stagnant point oblique flow of a Casson nanofluid with convective fluid temperature on the surface while the ambient fluid has a constant temperature. Sohail Nadeem *et al.* [2014] discussed the steady MHD three dimensional boundary layer flow of a Casson nanofluid past a linearly stretching with convective condition along the surface. Mahanta and Shaw [2015] analyzed the 3 dimensional MHD Casson fluid flows past a porous linearly stretching sheet with convective boundary condition. Mukopadhyay *et al.* [2014] studied the boundary layer flow of a Casson fluid over an exponentially stretching under the influence of a magnetic field, thermal radiation and suction/injection. The surface is prescribed by an exponential heat flux.

In recent years the theoretical study of effects of Hall current on MHD flows has been a subject of great interest due to its widely spread applications in power generators and pumps, Hall accelerators, refrigeration coils, electric transformers, in flight MHD, solar physics involved in the sunspot development, the solar cycle, the structure of magnetic stars, electronic system cooling, fiber and granular insulation, oil extraction, thermal energy storage and flow through filtering devices and porous material regenerative heat exchangers. Usually Hall term representing the Hall current was ignored in applying Ohm's law, because it has no remarkable effect for small and moderate values of magnetic field, The effects of Hall current are very important if a strong magnetic field is applied (Cramer, 1973), because, for a strong magnetic field the electromagnetic force is noticeable. The recent investigations for the applications of MHD are towards a strong magnetic field, due to which study of Hall current becomes significant.

The studies on fluid flows over an exponentially stretching surface with Hall currents in literature are very limited. Aziz and Nabil [2012] presented the effect of thermal radiation on steady MHD mixed convection flow past an exponentially stretching sheet with Hall currents assigning wall temperature and stretching velocity to vary according to specific exponential forms. Youcef Arirat and Kamel Handache [2014] studied the effect of Hall currents and thermal convection on the electrically conducting micropolar fluid. They proved that long – time and large date existence of a weak solution with decreasing energy to the system posed in a bounded domain along with initial boundary conditions. The studies on Casson fluid flows with Hall currents are very few. Afikuzzaman *et al* [2015] studied the effects of Hall currents on the unsteady Casson fluid flow through a parallel plate channel by maintaining constant temperatures on the plates subject to a transverse magnetic field. One of the plates is taken as stationary and the other plate is moving with an exponentially decaying pressure gradient along the flow direction.

To the best of the knowledge of the authors no study on the heat and mass transfer flow of a Casson fluid with convective heat flux on the surface is available In this chapter we made an attempt to analyse the influence of thermal radiation, temperature dependent heat source on the unsteady boundary layer flow heat and mass transfer of a Casson fluid over an exponentially stretching sheet with Hall currents with first order chemical reaction.

2 MATHEMATICAL FORMULATION

Consider the flow of an incompressible Casson fluid past a flat sheet which coincides with the plane y = 0. The fluid flow is confined to y > 0. Two equal and opposite forces are applied along the x-axis, so that the wall is stretched keeping the origin fixed. The stretching surface has the velocity $U_w(x, t) = \frac{U_0}{(1-\alpha t)} e^{x/L}$, α is a positive constant with dimension reciprocal time, L is the reference length, t is the time, We consider the convective heating process and hence the temperature on the surface shall be determined. The concentration at the surface C_w and the ambient value C_∞ attained as y tends to infinity are assumed to take constant values. A uniform magnetic field of strength B is applied normally to the stretching surface which produces magnetic effect in the x-axis. The effect of the induced magnetic field is neglected by taking a small magnetic Reynolds number.The effect of Hall current is to generate a force in the z – direction, which results in a cross flow in that direction, and hence the flow becomes three – dimensional. To simply the problem, we assume that there is no variation of flow variables in the z – direction; this assumption is valid if the plate would be of infinite extent in this direction. The generalized Ohm's law including Hall currents is given by

$$J = \sigma(E + V \times B - \frac{1}{en_e}J \times B + \frac{1}{en_e}\nabla P_e) \tag{1}$$

where $J = (J_x, J_y, J_z)$ is the current density vector, V is the velocity vector, E is the intensity vector of the electric field vector, **B** = (0, B, 0) is the magnetic induction vector, $\sigma(\sigma = \frac{e^2 n_e t_e}{m_e})$ is the electrical conductivity, t_e is the electron collision time, e is the electron charge, n_e is the electron number density, m_e is the mass of electrons and P_e is the electron pressure. In addition, there is no applied electric field in this work. The equation of conservation of electric charge $\nabla.J = 0$ results in $J_y = $ constant, this indicates that $J_y = 0$ every-where in the flow.
Hence (1) reduces to

$$J_x = \frac{\sigma B}{(1+m^2)}(mu - w) \tag{2}$$

$$J_z = \frac{\sigma B}{(1+m^2)}(u + mw) \tag{3}$$

where (u, v, w) are the velocity components in the (x, y, z) directions respectively, m $(= \omega_e t_e)$ is the Hall parameter, ω_e is the electron frequency.

The continuity, momentum, energy and concentration equations governing such type of flow invoking the Boussinesq's approximation can be written as

$$\frac{\partial u}{\partial x} + \frac{\partial v}{\partial y} = 0 \tag{4}$$

$$\frac{\partial u}{\partial t} + u\frac{\partial u}{\partial x} + v\frac{\partial u}{\partial y} = (1 + \frac{1}{\beta})\nu\frac{\partial^2 u}{\partial y^2} + g\beta(T - T_\infty) + g\beta^*(C - C_\infty) - \frac{\sigma B^2}{\rho(1+m^2)}(u + mw) \tag{5}$$

$$\frac{\partial w}{\partial t} + u\frac{\partial w}{\partial x} + v\frac{\partial w}{\partial y} = (1 + \frac{1}{\beta})\nu\frac{\partial^2 w}{\partial y^2} + \frac{\sigma B^2}{\rho(1+m^2)}(mu - w) \tag{6}$$

$$\frac{\partial T}{\partial t} + u\frac{\partial T}{\partial x} + v\frac{\partial T}{\partial y} = \frac{K}{\rho c_p}\frac{\partial^2 T}{\partial y^2} - \frac{1}{\rho c_p}\frac{\partial q_r}{\partial y} + \frac{Q_0}{\rho c_p}(T - T_\infty) \tag{7}$$

$$\frac{\partial C}{\partial t} + u\frac{\partial C}{\partial x} + v\frac{\partial C}{\partial y} = D\frac{\partial^2 C}{\partial y^2} - k(C - C_\infty) \tag{8}$$

The boundary conditions are

$$u = U_w(x, t), v = -V_w(x, t), w = 0, -K\frac{\partial T}{\partial y} = h_w(T_f - T) \ C = C_w(x, t) \text{ at } y = 0 \tag{9}$$

$$u \to 0, w \to 0, T \to T_\infty, C \to C_\infty \text{ as } y \to \infty \tag{10}$$

where u, v are the fluid velocity components along x and y axes respectively, ν is the kinematic viscosity, g is the gravity field, β_T is the volumetric coefficient of thermal expansion, β_C is the coefficient of expansion with concentration, ρ is the density of the fluid, $\beta = \mu_B \sqrt{2\pi_c}/P_y$ is parameter of the Casson fluid, T is the fluid temperature, C is the fluid concentration, σ is the electrical conductivity, c_p is the specific heat at constant pressure, K is the thermal conductivity of the medium, q_r is the radiation heat flux, Q_0 is the uniform volumetric heat generation and absorption, D is the mass diffusivity, k is the chemical reaction, $V_w(x, t) = f_w \left(\frac{U_0 \nu}{2L(1-\alpha t)} \right)^{1/2} e^{x/2L}$ is the velocity of suction $(V_w > 0)$, $f_w \geq 0$ is the suction parameter

We introduce the stream function $\psi(x, y)$ such that $u = \frac{\partial \psi}{\partial y}$ and $v = -\frac{\partial \psi}{\partial x}$.

The governing partial differential equations (5) - (8) can be reduced to a set of ordinary differential equations on introducing the following similarity variables:

$$\eta = \sqrt{\frac{U_0}{2\nu L(1-\alpha t)}} e^{x/2L} y, \qquad w = \frac{U_0}{(1-\alpha t)} e^{x/L} h(\eta), \tag{11}$$

$$\psi(x, y) = \sqrt{\frac{2U_0 \nu L}{(1-\alpha t)}} e^{x/2L} f(\eta), \tag{12}$$

$$\theta = \frac{T-T_\infty}{T_f - T_\infty}, \quad \phi = \frac{C-C_\infty}{C_w - C_\infty} \tag{13}$$

$$B^2 = B_0^2 (1-\alpha t)^{-1} \tag{14}$$

where B_0 is the magnetic field flux density.

Using (11) - (14) in equations (5) - (8) we obtain the following set of ordinary differential equations:

$$\left(1 + \frac{1}{\beta}\right) f''' + ff'' - 2f'^2 - e^{-X}\left(A(2f' + \eta f'') + \frac{2M}{1+m^2}(f' + mg)\right) + (G_r \theta + G_c \phi) = 0 \tag{15}$$

$$\left(1 + \frac{1}{\beta}\right) g'' + fg' - 2f'g + \frac{2M}{1+m^2}(mf' - g) = 0 \tag{16}$$

$$\theta''\left(1 + \frac{4}{3}Nr\right) + Pr\left(f\theta' - e^{-X}A\eta\theta' + \delta\theta\right) = 0 \tag{17}$$

$$\phi'' + Sc\left(f\phi' - e^{-X}A\eta\phi' - \gamma\phi\right) = 0 \tag{18}$$

The corresponding boundary conditions are

$$\eta = 0: \ f = f_w, \ f' = 1, \ g = 0, \theta'(0) = -Bi(1 - \theta), \ \phi = 1,$$
$$\eta \to \infty: f' \to 0, \ g \to 0, \ \theta \to 0, \ \phi \to 0, \tag{19}$$

Where the primes denote the differentiation with respect to η, $X = x/L$ is the dimensionless coordinate, $A = \alpha L/U_0$ is the unsteadiness parameter, $M = \sigma B_0^2 L/U_0 \rho$ magnetic parameter, $G_r = g\beta_T \Delta TL/U_w^2$ is the thermal Grashof number, $G_c = g\beta_c \Delta TL/U_w^2$ is the Solutal Grashof number, $Pr = \rho c_p \nu/k$ is the Prandtl number, $Nr = 4\sigma^* T_\infty^3/Kk^*$ is the thermal radiation parameter, $Sc = \nu/D$ is the Schmidt number, $Bi = -h_w/k \sqrt{\nu/a}$ is the Biot number, $\gamma = kL/U_w$ is the Chemical reaction parameter, $\delta = Q_0 L/U_w \rho c_p$ is the heat generation $(\delta > 0)$ and absorption $(\delta < 0)$ parameter.

The major physical quantities of interest are the local skin friction, the local Nusselt number and the local Sherwood number and are defined respectively by

$$C_{fx} Re_x^{\frac{1}{2}} = 2\left(1 + \frac{1}{\beta}\right) f''(0), \ C_{fz} Re_x^{\frac{1}{2}} = 2\left(1 + \frac{1}{\beta}\right) g'(0) \tag{19}$$

$$Nu_x Re_x^{-\frac{1}{2}} = -\theta'(0) \ and \ Sh_x Re_x^{-1/2} = \phi'(0) \tag{20}$$

3 RESULTS AND DISCUSSION

The objective of the present analysis is to understand the effects of Hall currents and chemical reaction on the unsteady flow of a Casson incompressible fluid past an exponentially stretching sheet in the presence of temperature dependent heat source and thermal radiation with convective boundary condition. The non –linear coupled equations governing the flow are solved by the Runge-Kutta fourth order method along with the shooting technique. To validate the accuracy of the numerical scheme the present results are compared with those of Elbashbeshy et al. (2012), Ishak (2011) viz., $-\theta'(0)$ in the absence of Hall currents and concentration in the unsteady case and for the corresponding steady case with those of and with Kameswaran (2012) i.e. $-f''(0)$ in the absence of suction, Hall parameter, thermal and solutal buoyancy, heat generation/absorption and Prandtl number for a steady flow. $X = A = Gr = Gc = \delta = m = Ec = Nr = fw = Bi = \phi = 0$ for different values of M and Pr. The compared values of $-\theta'(0)$ and $-f''(0)$ are presented in Tables 1 and 2 which are found to be in good agreement with the said published results.

Table 1: Comparison of the values of $-f''(0)$ for various values of M with
$m = A = \delta = Gr = Gc = \beta = Pr = Nr = Sc = \gamma = fw = Bi = 0$

M	Kameswaran[2012]	Present results
0	1.28181	1.281857
1	1.62918	1.629178
2	1.91262	1.912624
3	2.15874	2.158742

Table 2: Comparison of the values of $-\theta'(0)$ for various values of Pr with
$M = m = Gr = Gc = \beta = Nr = Sc = \gamma = fw = Bi = 0$

Pr	Elbashbeshy et al [2012]	Ishak [2011]	Present results
1.0	0.95478	0.9547	0.9547
2.0	1.47146	1.4714	1.4714
3.0	1.86907	1.8691	1.86907
5.0	2.50013	2.5001	2.5001
10.0	3.66.37	3.6603	3.66035

In order to analyze the effects Casson parameter, Hall current, thermal buoyancy force, solutal buoyancy force, chemical reaction, heat source/absorption, thermal radiation, convective heat at the boundary and unsteadiness on the flow-field, the computational values of the flow variables are presented graphically and discussed for various values of the governing parameters.

The influence of the Casson parameter is plotted in Figs. 1 – 4. It is noticed that Casson parameter enhances both the velocities decreases. The associated boundary layers are thinner. In the unsteady case the flow rate is faster than in steady case. The primary velocity from its peak value on the boundary decreases asymptotically eventually attaining the free stream value. The secondary velocity increases rapidly in vicinity of the boundary attain its maximum value then decreases to attain the free stream value. As β increases the secondary velocity increases in the vicinity of the boundary and attains the peak value and subsequently the secondary velocity decreases with β and reaches its free stream value. The temperature increases with β in the steady case with enlarged thermal boundary layers while in the unsteady case the increase is very small. The effect of the Casson parameter on mass concentration is similar to that of temperature.

Fig. 5 shows that the primary velocity reduces throughout the boundary layer region with increasing values of magnetic parameter. The deceleration in the velocity is owing to the retarding nature of the Lorentz force. From Fig. 6 it is noted that secondary velocity increases rapidly near the plate attaining maximum value and then decreases in the rest of the region eventually approaching the free stream value. The secondary velocity significantly increases with the magnetic field unlike the primary velocity. The peak value of the secondary velocity when M = 0.8 is two and half times to that corresponding to M = 0.2. Figs. 7 and 8 indicate that the temperature and concentration increase nominally with increasing values of magnetic parameter.

Fig. 9 and Fig. 10 show the effect of Hall current on the primary velocity and secondary velocity. It is observed that on increasing Hall parameter (m) the primary velocity enhances showing an increase in the transport while the secondary velocity increases significantly throughout boundary layer region. It may be said that Hall current tends to accelerate the fluid throughout the boundary layer region which is in conformity with the fact that the secondary velocity arises due to Hall currents.

Figs. 11 – 14 depict the effect of thermal and solutal buoyancy forces on the primary and secondary velocities. It is observed that both the velocities increase on increasing Gr and Gc as the thermal and concentration buoyancy forces accelerate both the velocities throughout the boundary layer region. Fig. 15 reveals that for increasing values of Biot number the temperature is enhanced predominantly on the surface as expected owing to the strong convection. The corresponding temperature profiles are steep near the boundary.

Fig. 16 implies that reduction in the temperature for increasing values of Pr is expected as a result of decreasing thermal conductivity. Fig. 17 shows that the temperature is found to be an increasing function of thermal radiation which facilitates additional means to diffuse energy as an enhancement in the radiation parameter which corresponds to a reduction in the Rosseland mean absorption coefficient K^* for fixed values of T_∞ and k. The associated thermal boundary layers are thicker.

From Fig. 18 the presence of heat source is found to enhance the temperature owing to the release of energy in the thermal boundary layer and the associated thermal boundary layers are thicker. On increasing $\delta > 0$ the temperature further rises. In the case of heat absorption, $\delta < 0$ (heat sink) the temperature falls with decreasing values of $\delta < 0$ owing to the absorption of energy in the thermal boundary layer.

From Fig. 19 the species concentration is observed to reduce with increasing values of the Schmidt number throughout the region which is associated with thinner solutal boundary layers. Thus the mass transfer rate is enhanced.

The influence of chemical reaction rate parameter γ on the species concentration for generative chemical reaction is depicted in Fig. 20. It is found that species concentration with its highest value at the plate decreases slowly till it reaches the minimum value i.e., zero at the far downstream. Further, increasing of the chemical reaction parameter decreases concentration of species in the boundary layer due to the fact that destructive chemical reduces the thickness of the solutal boundary layer and increases the mass transfer.

The influence of suction/injection f_w on the velocity, temperature distributions are plotted in Figs. 21 – 24. It is observed that primary velocity decreases with increasing suction parameter and the injection (blowing) accelerates the flow. The wall suction($f_w > 0$) results in thinner boundary layers with a fall in the velocity. For blowing ($f_w < 0$) an opposite trend is noticed. The behavior of the secondary velocity with f_w is similar to that of the primary velocity. However, in this case the influence of f_w is stronger than that on primary velocity. $f_w = 0$ correspond to the impermeable stretching surface. From Fig. 23 it is revealed that the temperature enhances with blowing and diminishes with increasing suction parameter. It is evident from Fig. 24 that mass concentration also behaves similar to that of the temperature.

The skin friction coefficient, local Nusselt number and local Sherwood number for different values of the governing parameters are presented in Table 3. It is observed that increasing values of the unsteady parameter reduce the skin friction coefficient in both x and z directions. The rate of heat and mass transfer is found to decrease with increasing unsteady parameter. Higher the magnetic fields lessen the skin friction coefficient corresponding to the primary velocity and while it enhances the skin friction coefficient corresponding to the secondary velocity. The Nusselt and Sherwood numbers show a decreasing trend. The Hall parameter has an increasing influence on the skin friction coefficient in both x and z – directions, Nusselt number and Sherwood number. The thermal buoyancy and solutal buoyancy parameters enhance the skin friction coefficient in the x direction including the Nusselt and Sherwood numbers while the skin friction coefficient in the z direction gets depreciated. The Prandtl number depreciates the skin friction coefficient in the x and z-directions and the Sherwood number whereas the Nusselt number shows as increasing tendency. The Nusselt number is seen to decrease with increasing radiation parameter while the skin friction coefficient in both the directions and Sherwood number are found to enhance. The impact of heat source parameter shows qualitatively similar effect on these variables as that of the thermal radiation parameter. The influence of Schmidt number decreases the skin friction coefficient in both the directions. The Nusselt number reduces while the Sherwood number enhances with increasing Schmidt number. The increasing value of the Casson parameter enhances the skin friction coefficient in the z – direction while the skin friction coefficient in the x direction and the Sherwood number and the Nusselt number are reduced. The chemical reaction parameter decreases the skin friction coefficient and Nusselt number whereas the Sherwood number enhances. The suction parameter reduces the skin friction coefficient in the x-direction while it increases the skin friction coefficient in the z – direction. The Nusselt number and Sherwood number are seen to increase with f_w. The Biot number enhances the drag coefficients, Nusselt and Sherwood numbers.

Table 3: Skin friction, Nusselt number and Sherwood number values for variation of different parameters

β	A	M	m	Gr	Gc	Pr	Nr	δ	Sc	γ	fw	Bi	$f''(0)$	$g'(0)$	$-\theta'(0)$	$-\phi'(0)$
0.2													-0.878855	0.159569	0.095053	0.776283
0.4	0.1	0.5	0.5	1.0	1.0	0.72	0.5	0.1	0.5	0.5	0.5	0.1	-1.125859	0.218099	0.087439	0.760453
0.6													-1.283979	0.254328	0.085795	0.752010
	2.0												-1.788964	0.112153	0.095850	2.962392
2.0	4.0	0.5	0.5	1.0	1.0	0.72	0.5	0.1	0.5	0.5	0.5	0.1	-2.337888	0.097930	0.096946	3.981809
	6.0												-2.773158	0.088837	0.097464	4.779501
		0.1											-0.712298	0.037834	0.078478	0.481880
2.0	0.1	0.3	0.5	1.0	1.0	0.72	0.5	0.1	0.5	0.5	0.5	0.1	-0.811060	0.100536	0.077142	0.469695
		0.5											-0.904503	0.151148	0.075633	0.458428
			0.1										-1.421002	0.010972	0.136911	0.449323
2.0	0.1	0.5	0.3	1.0	1.0	0.72	0.5	0.1	0.5	0.5	0.5	0.1	-1.412522	0.024002	0.138980	0.450240
			0.6										-1.396512	-0.004497	0.146014	0.452358
				0.5									1.094179	-0.148071	0.083017	0.579253
2.0	0.1	0.5	0.5	1.0	1.0	0.72	0.5	0.1	0.5	0.5	0.5	0.1	1.065348	-0.149746	0.083230	0.582734
				0.5									1.037529	-0.151297	0.083419	0.585979
					0.5								-1.532449	-0.002420	0.130245	0.428824
2.0	0.1	0.5	0.5	1.0	1.0	0.72	0.5	0.1	0.5	0.5	0.5	0.1	-1.401045	0.013103	0.143133	0.451659
					0.5								-1.273830	0.014800	0.155363	0.469672

2.0	0.1	0.5	0.5	1.0	1.0	0.72	0.5	0.1	0.5	0.5	0.5	0.1	-0.789618	0.086074	0.078075	0.472131
						1.0							-0.814705	0.085062	0.083469	0.467542
						3.0							-0.850941	0.084076	0.092234	0.462684
2.0	0.1	0.5	0.5	1.0	1.0	0.72	1.0	0.1	0.5	0.5	0.5	0.1	-0.947347	0.120896	0.062200	0.448468
							2.0						-0.939687	0.121872	0.058937	0.450870
							3.0						-0.936627	0.122290	0.057676	0.451884
2.0	0.1	0.5	0.5	1.0	1.0	0.72	0.5	-1.0	0.5	0.5	0.5	0.1	-1.006799	0.141168	0.091463	0.646712
								0.0					-0.962752	0.144476	0.081054	0.650721
								0.5					-0.693379	0.152224	0.011963	0.668568
2.0	0.1	0.5	0.5	1.0	1.0	0.72	0.5	0.1	0.1	0.5	0.5	0.1	-0.559280	0.035698	0.081510	0.198091
									0.2				-0.587417	0.034372	0.080785	0.286219
									0.3				-0.608308	0.033369	0.080102	0.360678
2.0	0.1	0.5	0.5	1.0	1.0	0.72	0.5	0.1	0.5	-0.1	0.5	0.1	-0.780677	0.130850	0.077458	0.323802
										0.0			-0.792130	0.129034	0.076666	0.400686
										0.1			-0.926834	0.110732	0.106662	0.423110
2.0	0.1	0.5	0.5	1.0	1.0	0.72	0.5	0.1	0.5	0.5	-0.5	0.1	-0.486994	0.149892	0.079658	0.662248
											0.0		-0.631822	0.154953	0.083232	0.785241
											0.5		-0.803743	0.155852	0.086107	0.925768
2.0	0.1	0.5	0.5	1.0	1.0	0.72	0.5	0.1	0.5	0.5	0.5	0.05	-0.817403	0.085906	0.043255	0.467491
												0.1	-0.783389	0.086835	0.127174	0.472094
												0.2	-0.736954	0.087998	0.127174	0.477957
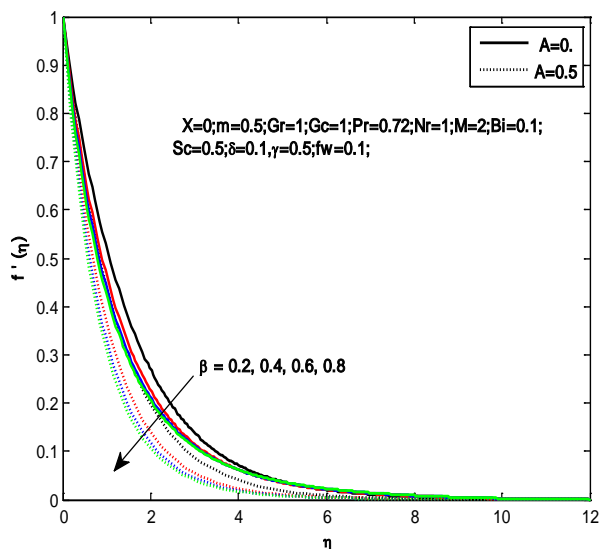
Fig. 1: Primary Velocity profiles for different Values of β
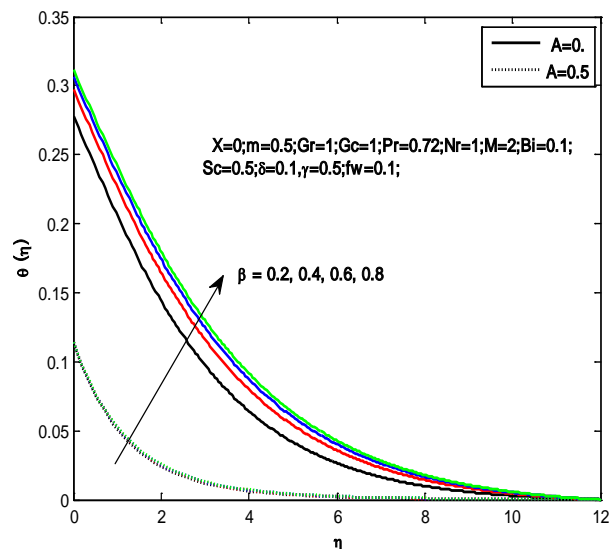
Fig. 3: Temperature profiles for different Values of β
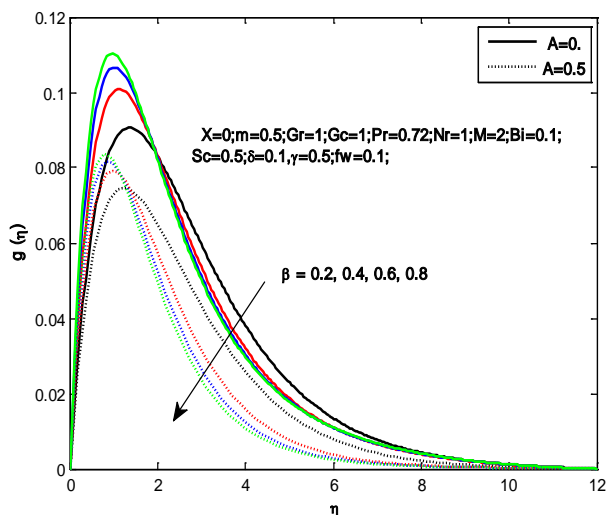
Fig. 2: Secondary Velocity profiles for different Values of β
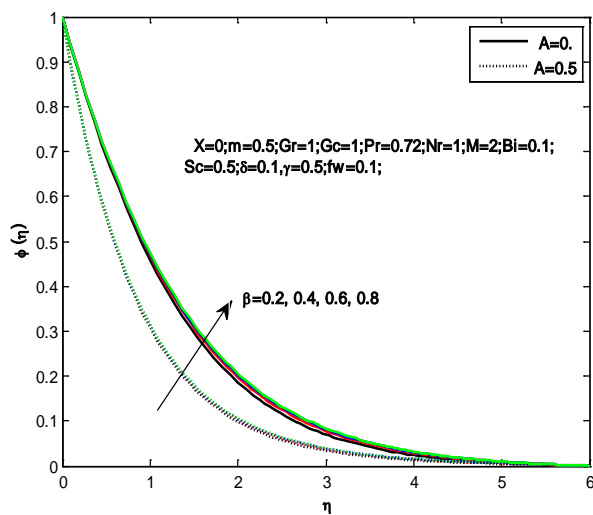
Fig. 4: Concentration profiles for different Values of β
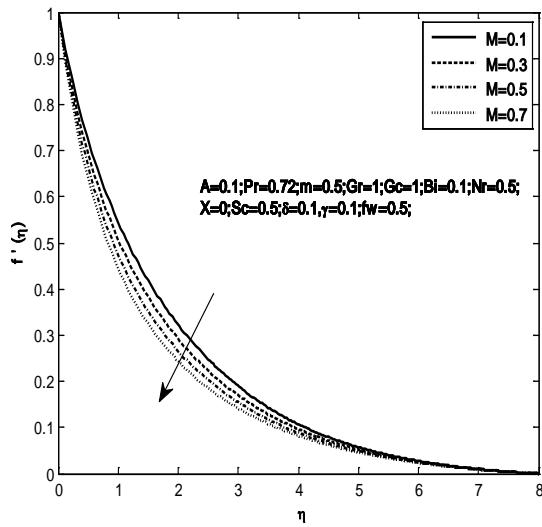
Fig. 5: Primary Velocity profiles for different Values of M
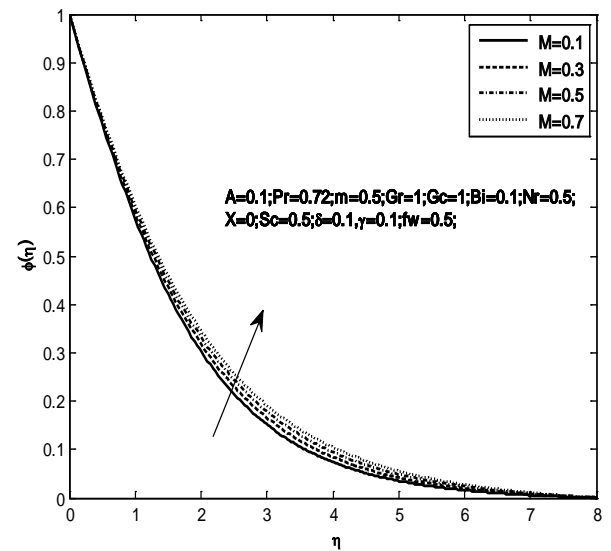
Fig. 8: Concentration profiles for different Values of M
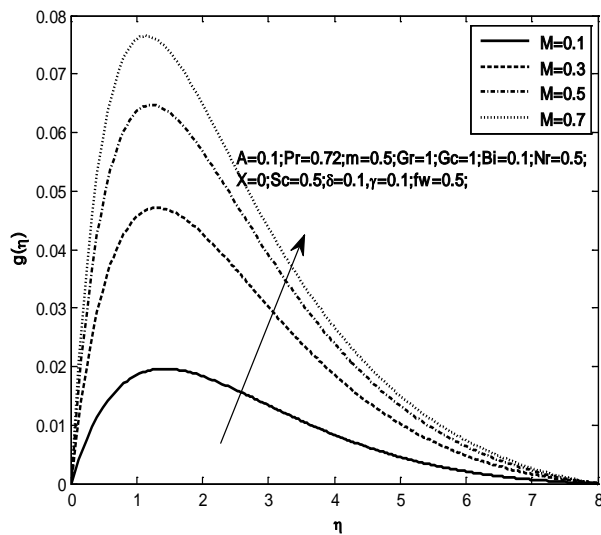
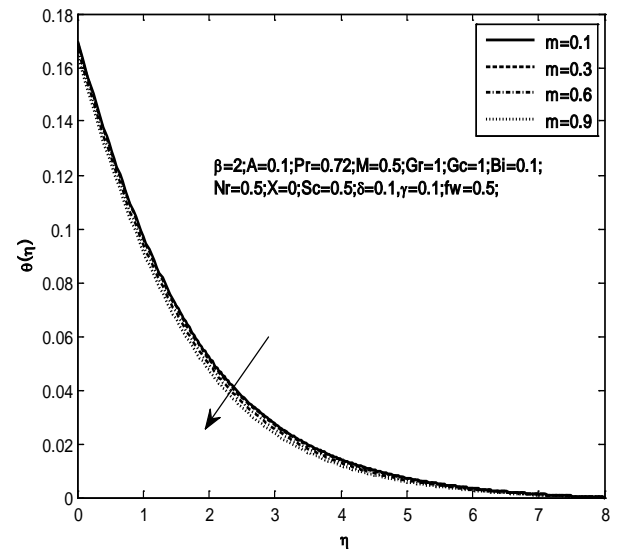**Fig. 6:** Secondary velocity profiles for different Values of M

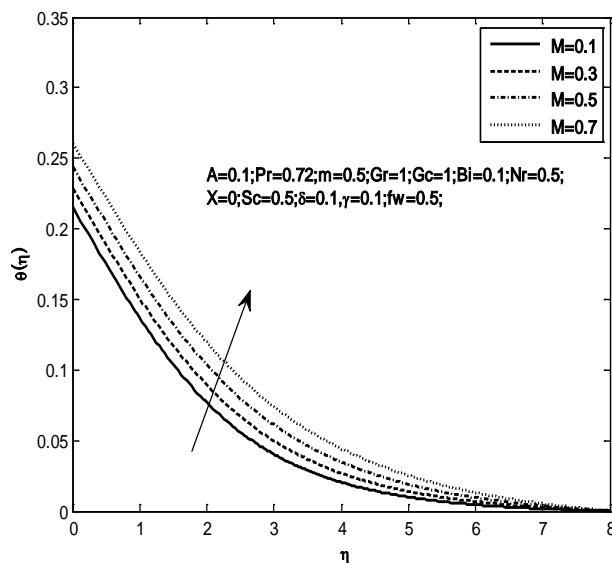**Fig. 9:** Temperature profiles for different Values of m

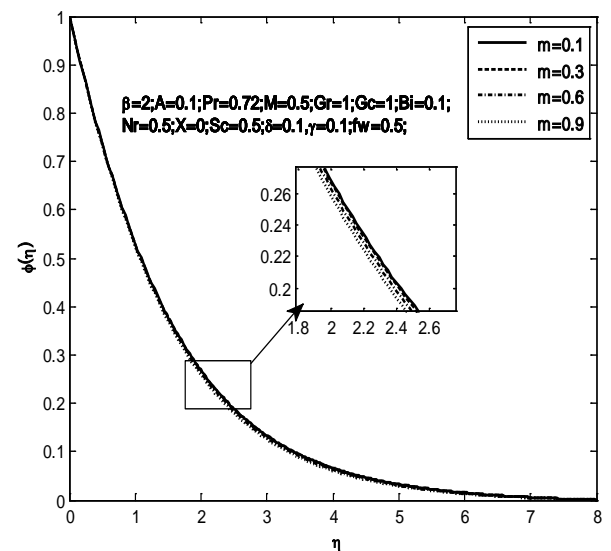**Fig. 7:** Temperature profiles for different Values of M

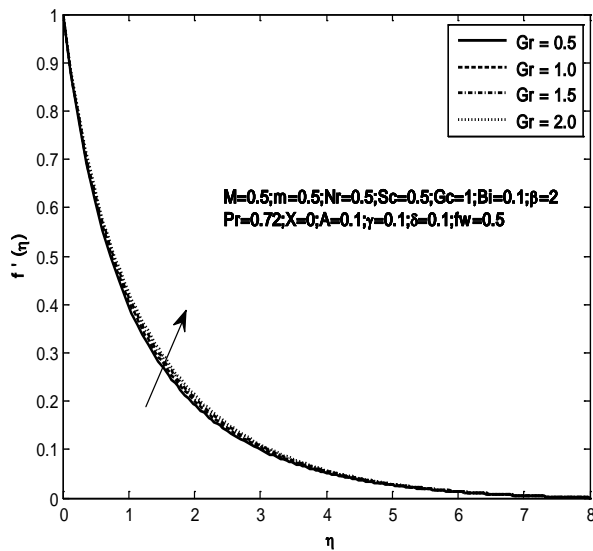**Fig. 10:** Concentration profiles for different Values of m

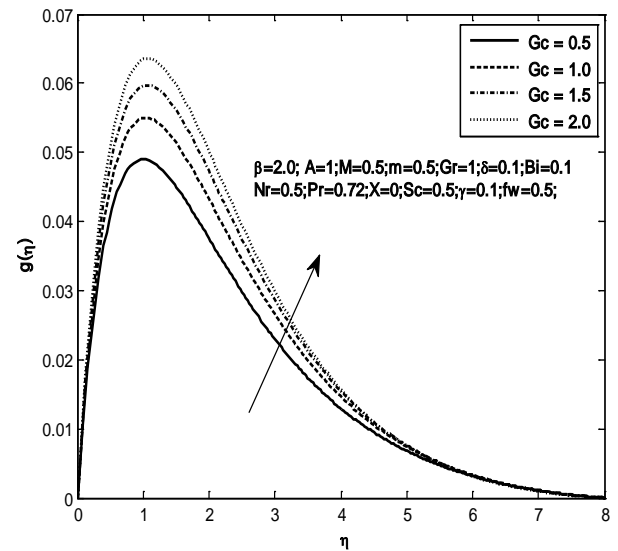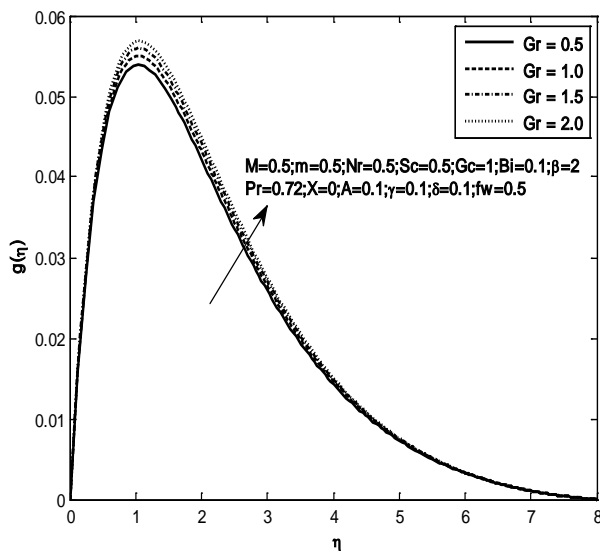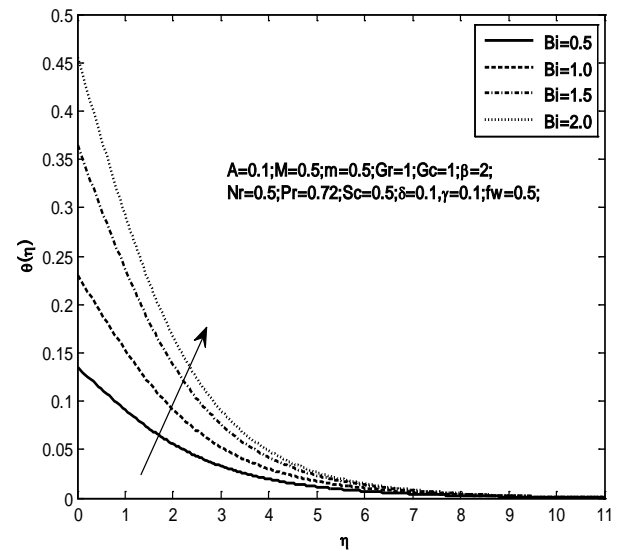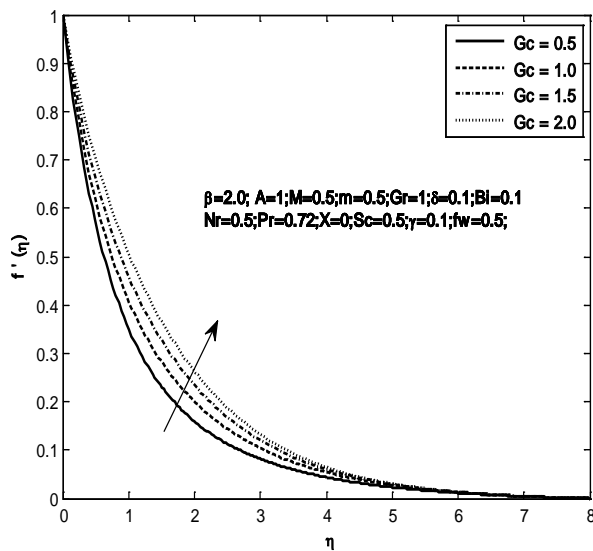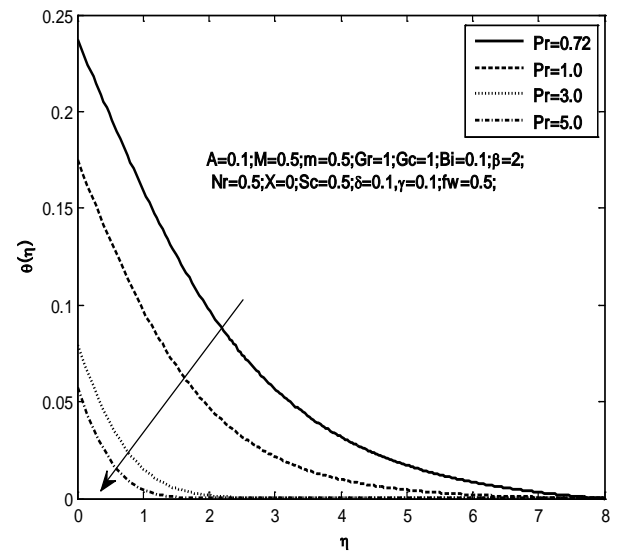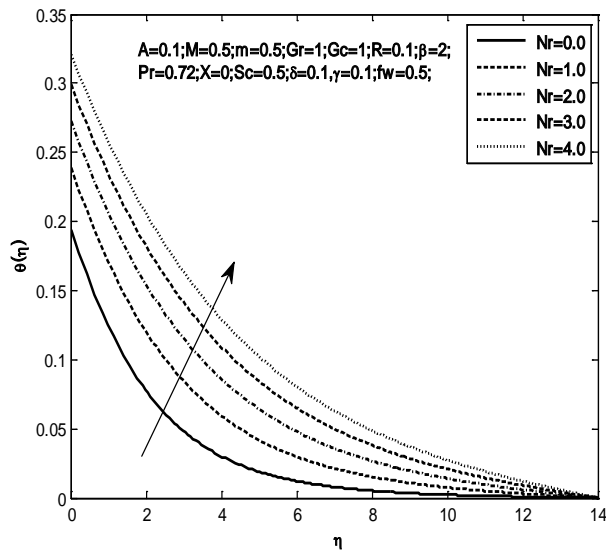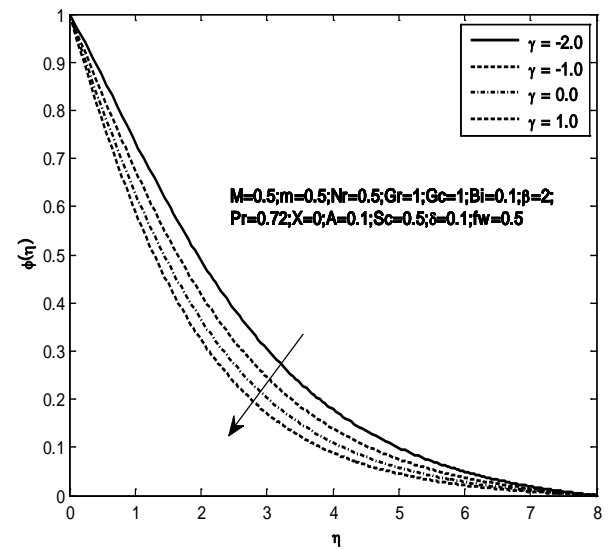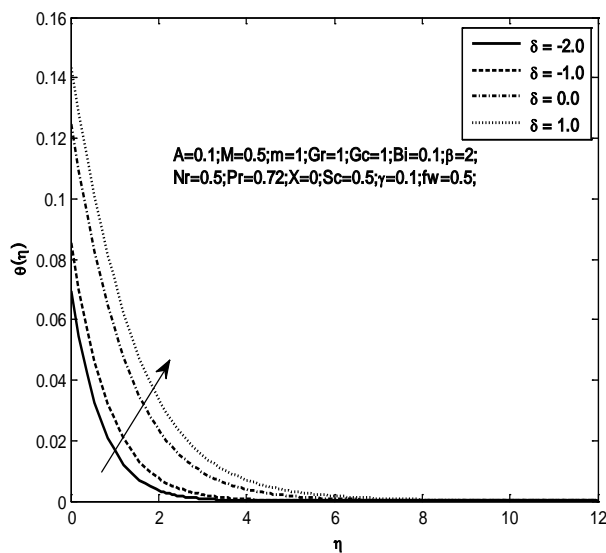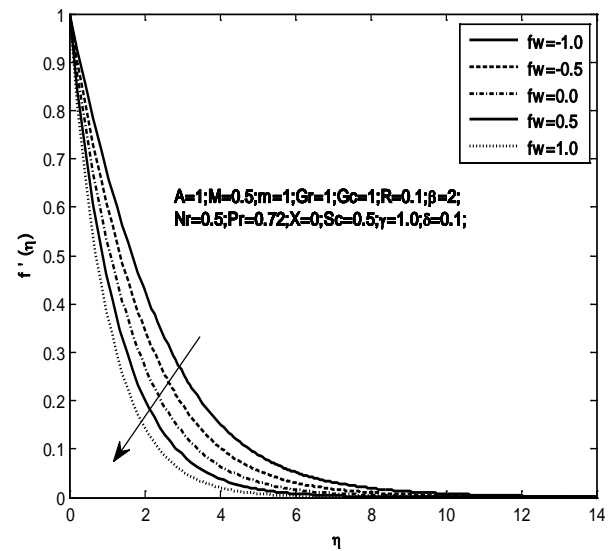**Fig. 11:** Primary velocity profiles for different Values of Gr

Fig. 14: Secondary velocity profiles for different Values of Gc

Fig. 12: Secondary velocity profiles for different Values of Gr

Fig. 15: Temperature profiles for different Values of Bi

Fig. 13: Primary velocity profiles for different Values of Gc

Fig. 16: Temperature profiles for different Values of Pr

Fig. 17: Temperature profiles for different Values of Nr

Fig. 20: concentration profiles for different Values of γ

Fig. 18: Temperature profiles for different Values of δ

Fig. 21: Primary velocity profiles for different Values of fw
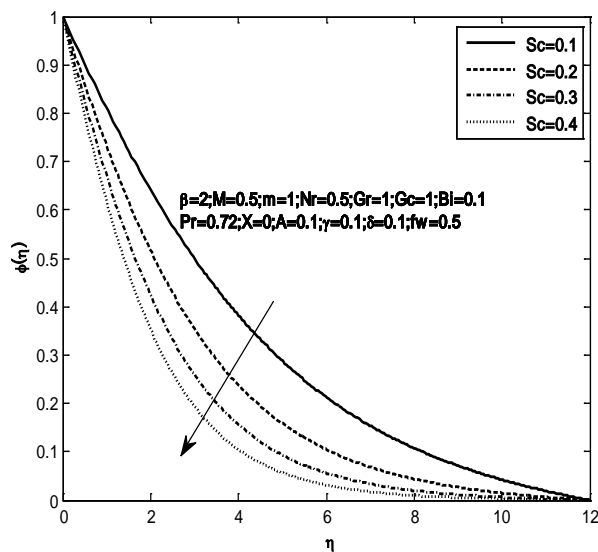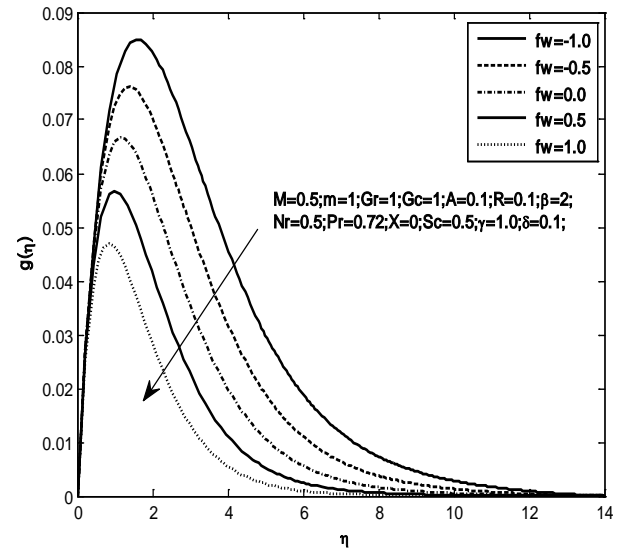

Fig. 19: Concentration profiles for different Values of Sc

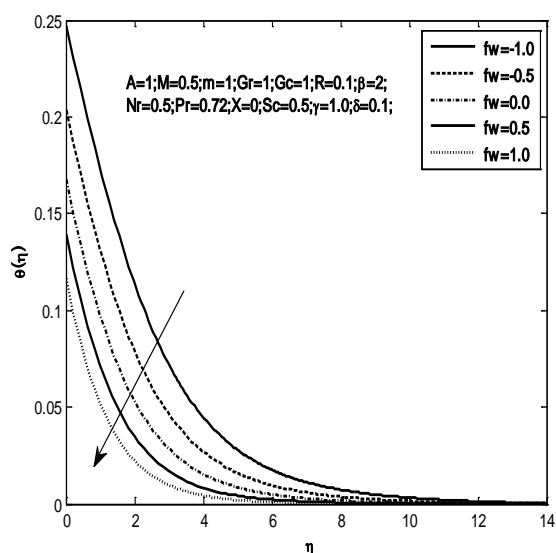**Fig. 22:** Secondary velocity profiles for different Values of fw

Fig. 23: Temperature profiles for different Values of fw
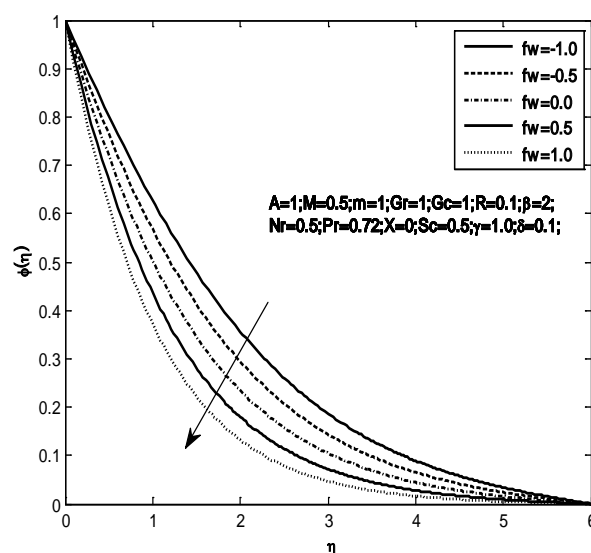

Fig. 24: Concentration profiles for different Values of fw

4 CONCLUSIONS

The unsteady boundary layer flow of an incompressible Casson fluid over an exponentially stretching sheet in the presence of thermal radiation, temperature dependent heat source and Biot number with chemical reaction and Hall currents is analysed. It is observed that the primary velocity decreases with Casson parameter, unsteady parameter, suction and magnetic field parameter while an opposite trend is noted with blowing and Hall parameter. The secondary velocity follows an opposite effect to that of primary velocity for variation of magnetic parameter. The temperature and concentration distributions increase with increasing magnetic field parameter and decrease with Hall parameter. The thickness of the thermal boundary layer increases with increasing values of radiation parameter and heat generation parameter while a reduction is noticed with suction parameter. The mass transfer rate decreases with Schmidt number and chemical reaction parameter.

5. REFERENCES

[1] Afikuzzaman Md., Ferdows M. and Mahmud Alam Md., Unsteady MHD Casson fluid flow through a parallel plate with Hall current, Procedia Engineering, 105 (2015), 287 – 293.

[2] Anwar Beg O., Khan M.S., Karim I., Alam M. and Fredows M., Explicit numerical study of unsteady hydromagnetic mixed convective nanofluid flow from an exponentially stretching sheet in porous media, Applied Nano Science, 4 (2014), 943 – 957.

[3] Aziz M. A. E. and Nabil, T., Homotopy analysis solution of hydromagnetic mixed convection flow past an exponentially stretching sheet with Hall current, Mathematical Problems in Engineering, doi: 10.1155/454023, (2012).

[4] Cramer K. and Pai S. Magnetofluid dynamics for Engineers and Applied Physicists Mc. Graw-Hill, New York, (1973)

[5] Elbashbeshy E. M. A., Emam T. G. and Abelgaber K. M., Effects of thermal radiation and magnetic field on unsteady mixed convection flow and heat transfer over an exponentially stretching surface with suction in the presence of internal heat generation/absorption, Journal of Egyptian Mathematical Society, 20 (2012), 215 – 222.

[6] Ishak A., MHD boundary layer flow due to an exponentially stretching sheet with radiation effect, Sains Malaysiana, 40 (2011), 391-5.

[7] Kameswaran P. K., Narayana M., Sibanda P. and Makanda G., On radiation effects on hydromagnetic Newtonian liquid flow due to an exponential stretching sheet, Boundary Value Problems, 105 (2011)

[8] Magyari E. and Keller B., Heat and mass transfer in the boundary layers on an exponentially stretching continuous surface, J. Phys. Appl. Phys. 32 (1999), 577 – 585.

[9] Mahanta G. and Shaw S., 3D Casson fluid flow past a porous linearly stretching sheet with convective boundary condition, Alexandria Engineering Journal, 54 (2015), 653 – 659.

[10] Mukhopadyay S., Iswar Chandra Moindal. and Hayat T., MHD boundary layer flow of a Casson fluid passing through an exponentially stretching permeable surface with thermal radiation, Chinese Phys. B, 23(10) (2014), 104701.

[11] Nadeem S. and Hussain S. T., Heat transfer analysis of Williamson fluid over an exponentially stretching surface, Appl. Math. Mech. – Engl. Ed., 35(4) (2014), 489 – 502.

[12] Nadeem S., Rashid Mehmood and Noren Sher Akbar, Optimezed analytical solution for oblique flow of a Casson-nano fluid with convective boundary conditions" Internal Journal of Thermal Science, 78 (2014), 90 – 100.

[13] Nadeem S., Zaheer S. and Fang T., Effects of thermal radiation on the boundary layer flow of a Jeffrey fluid over an exponentially stretching surface, Numer. Algor. 57 (2011), 187 – 205.

[14] Pavithra G. M. and Gireesha B. J., Effect of Internal Heat Generation / Absorption on Dusty Fluid Flow over an Exponentially Stretching Sheet with Viscous Dissipation, Journal of Mathematics, http://dx. doi. Org/ 10. 1155/2013/2013/583615, (2013)

[15] Sohail Nadeem, Rizwab Ul Haq and Noren Sher Akbar, MHD three dimensional boundary layer flow of Casson nano fluid past a linearly stretching sheet with convective boundary condition, IEEE Transactions on nanotechnology, 13(1) (2014)

[16] Youcef Arirat and Kamel Handache, Global weak solutions to the equations of thermal convection in micropolar fluids subjected to Hall current, Nonlinear Analysis, 102 (2014), 186 – 207.

Source of support: Nil, Conflict of interest: None Declared